

MICROSTRUCTURE AND MECHANICAL CHARACTERISTICS OF TITANIUM ALLOY TC21 AFTER HEAT TREATMENT

M. Abdelhameed¹, Ramadan N. Elshaer², Khaled M. Ibrahim³, A. Sobh⁴ & M. El-Shennawy⁵

¹*Research Scholar, Petrojet Co., Cairo, Egypt*

²*Research Scholar, Tabbin Institute for Metallurgical Studies, Cairo, Egypt*

³*Research Scholar, Central Metallurgical R&D Institute, Cairo, Egypt*

⁴*Research Scholar, Faculty of Engineering, Helwan University, Cairo, Egypt*

ABSTRACT

Effect of heat treatment on microstructure and mechanical properties of TC21 titanium alloy was investigated. TC21 in annealed condition with an equiaxed $\alpha+\beta$ structure was solution treated at temperature below β -transus (920°C , 15 min) and temperature above β -transus (1020°C , 15min, WQ). Aging was applied for both groups of samples (600°C , 4h, AC). Treated samples below β -transus showed an equiaxed $\alpha+\beta$ structure. Samples treated above β -transus have been changed to a solely β -phase with little amount of secondary α -phase precipitated in the formed β -phase due to high cooling rate and aging process. Maximum hardness of 492HV_{30} was reported for samples treated at 1020°C due to precipitation of secondary lamellar alpha phase and small lathes of martensitic phase (α') in β -matrix. Maximum tensile strength of 1447MPa and ductility of 8% were reported for the samples treated at 920°C due to its structure that contained α , β and α_s . Hence, treated samples at 920°C showed the best mechanical properties and the most reliable and repeatable characteristics.

KEYWORDS: *TC21 Titanium Alloy; Heat Treatment; Microstructure; Mechanical Properties*

Article History

Received: 21 Apr 2021 | Revised: 27 Apr 2021 | Accepted: 11 May 2021

INTRODUCTION

Titanium and its alloys are commonly used in manufacturing some parts of structure components and engine rotors for the aerospace industry and petroleum sector due to their high strength, low density, high corrosion resistance and low crack propagation [1]. The excellent balance of plasticity and fracture toughness with strength, attention has been paid to this titanium alloy; TC21 in the last decade [2-4].

Titanium alloy can be classified into three main categories according to microstructure; α , $\alpha+\beta$ and β alloys. $\alpha+\beta$ titanium alloys have the best properties compared to other categories. Nowadays, $\alpha+\beta$ titanium alloys are widely used in aerospace applications, aero-engines, petroleum sector and chemical industries [1-2, 5-6]. More than 50% of the used titanium alloys in different applications among $\alpha+\beta$ titanium category is Ti-6Al-4V alloy.

TC21 titanium alloy with a chemical composition (Ti-6 Al-2Sn-2 Zr-3 Mo-1 Cr-2 Nb-Si, wt. %) is another category of $\alpha+\beta$ titanium alloys that are mainly used in aircraft structure building application [2]. TC21 titanium alloy showed better mechanical properties than Ti-6Al-4V at room temperature. TC21Ti-alloy has tensile strength of more than 1100MPa [5] while Ti-6Al-4V has tensile strength in the range of 895Mpa to 933Mpa [7-8]. TC21 titanium alloy with equiaxed microstructure has lower crack growth than Ti-6Al-4V [4]. In addition, both ultimate and yield strengths decrease with increasing the content of coarse α -plates in the structure [9]. However, some studies showed that the best strength of TC21titanium alloy can be achieved with full β phase microstructure [10]. In other studies, it was found that excellent strength of TC21 titanium alloy was in the range of 800 Mpa [11-12].

The objective of this work is to investigate the effect of heat treatment on microstructure and mechanical properties of the annealed TC21 titanium alloy.

EXPERIMENTAL

The initial alloy in this work derived from the TC21 titanium alloy as hot-forged bars with diameter 7mm and length 140mm. Chemical composition of this alloy is Ti-6Al-3Mo-2Sn-2Nb-2Zr-1Cr-Si wt.%. The phase transus temperature was about 955°C [2, 13]. Original microstructure shown in Fig. 1 consists of equiaxed primary α_p phase (dark area) and β phase (gray area). The grain size of α -phase was in the range of 2.5 μ m and its volume fraction was approximately 65%. The equiaxed α phase was distributed homogeneously in the whole structure. The XRD pattern confirmed the presence of α and β phases in the as-received TC21 alloy as shown in Fig. 2. It is noticed that β peaks are rather weak, suggesting existing of a relatively low volume fraction of β phase (35%) [14-15].

The hot-forged TC21 alloy was solution treated above \square transus temperature (1020°C) and below \square transus temperature (920°C). The schematic of solution treatment and aging processes is shown in Fig. 3. Phase identification was carried out using X-ray diffraction (XRD). Hardness was measured using Vickers hardness tester. Five readings were taken on each sample and the average was recorded. Tensile tests were performed on machined samples with 4mm diameter and 20mm gage length. Fractographic features of some selected tensile samples were examined using field emission scanning electron microscope (FESEM) to study the fracture mechanics of the investigated TC21 titanium alloy

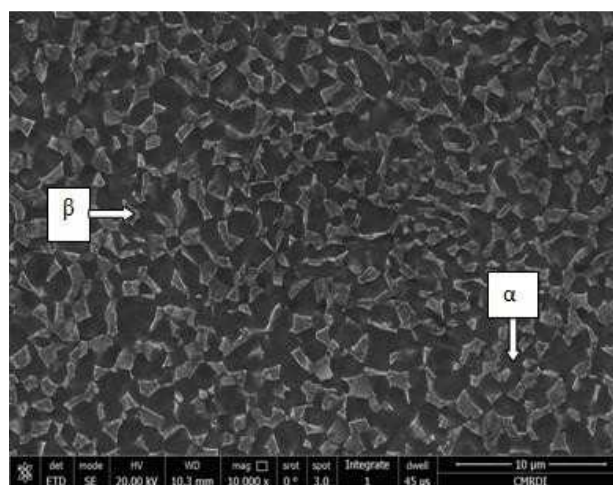


Figure 1: FESEM Micrograph of the as Received TC21 Titanium Alloy.

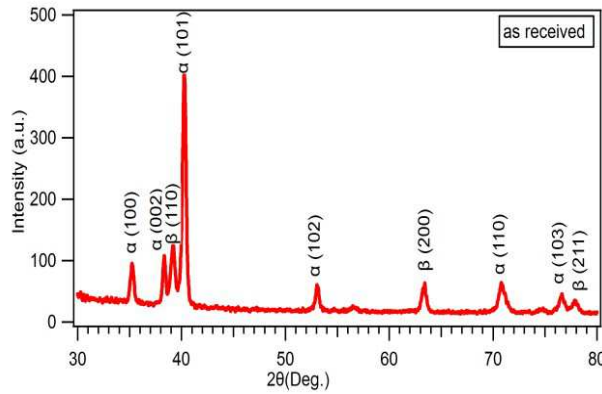


Figure 2: XRD Pattern of the As Received TC21 Titanium Alloy.

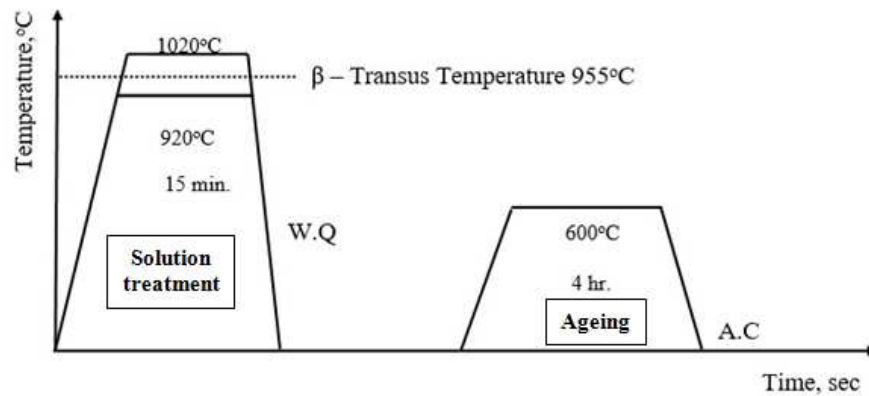


Figure 3: Schematic of Solution Treatment and Ageing Processes of TC21 Titanium Alloy.

RESULTS AND DISCUSSIONS

Microstructure Investigation

Figure4 (a) shows microstructure of heat treated sample below β -transus (920°C, 15 min, WQ) then aged at (600°C, 4hr). The microstructure contained α_p phase (primary equiaxed alpha phase, dark area) and β -phase (gray area) with a volume fraction of 25%. At higher magnification shown in Fig.4 (b), secondary lamellar α_s -plates (α_s), which appeared as lathes, was precipitated on the β -phase (as indicated by arrows) after applying aging process. The average grain size of β -grain increased relatively compared to the as-received condition, where it recorded a grain size of about 3 μ m. In addition, the size of α -phase was increased gradually with also coarsening of β -grains.

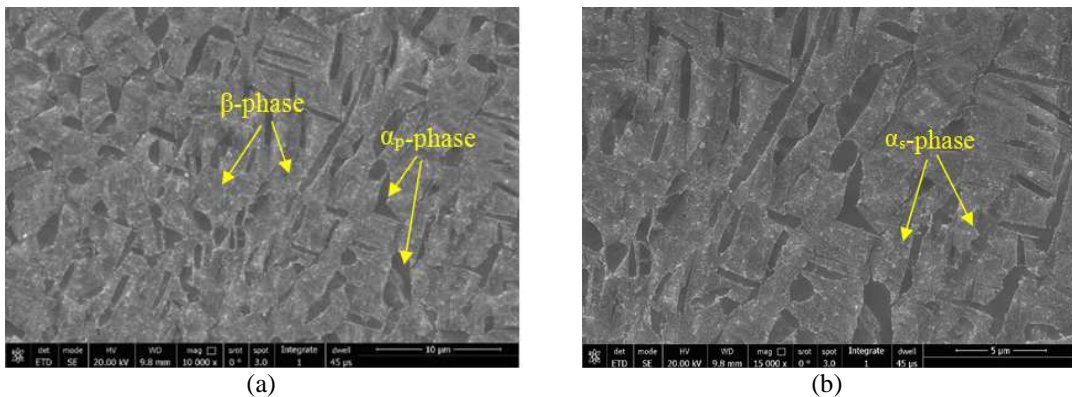


Figure 4: FESEM Micro Graph of Solution Treated Sample at 920°C.

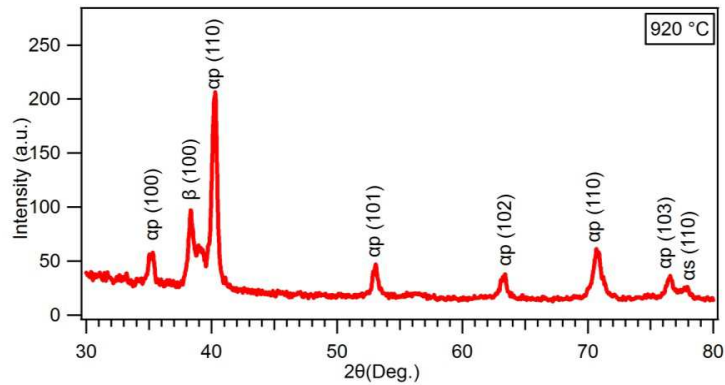


Figure 5: XRD Pattern of Solution Treated TC21 Sample at 920⁰C.

Figure 5 shows X-Ray diffraction pattern of the treated sample at 920⁰C. The patterns for the sample verified the above mentioned phases existing in the microstructure (*ap*, *as* and β phases). Figure 6 shows microstructure of the sample treated above β -transus temperature; (1020⁰C, 15min, WQ) then aged at (600⁰C, 4hr). The microstructure revealed that β -grains contained secondary lamellar α -plates (α_s) and martensitic phase (α^{\parallel}). A_s was precipitated due to aging process and α^{\parallel} due to quenching from high temperature during solution treatment at 1020⁰C. Solution temperature above the β -transus (1020⁰C) caused an increase in the average grain size of the β -grain compared to as-received and solution treated at 920⁰C conditions. The average grain size reached 300 μ m. It is obvious that the grain size of the sample solution treated at 1020⁰C was in the range of 100 to 120 times the other conditions (solution treated sample at 920⁰C and the as-received one).

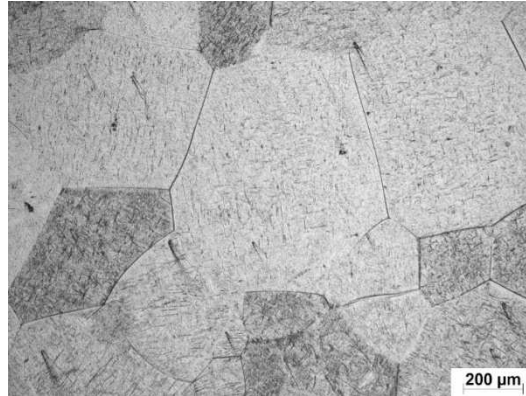


Figure 6: Optical Micro Graph of Solution Treated Sample at 1020⁰C.

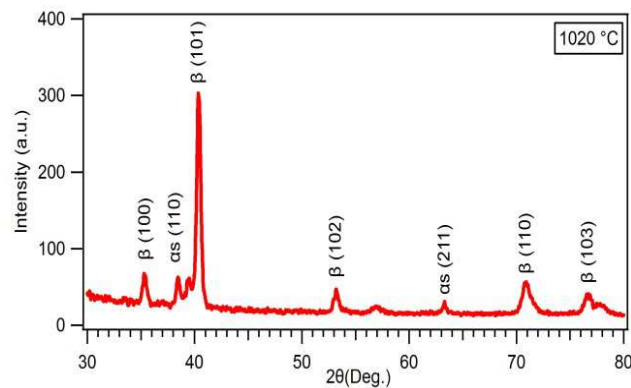


Figure 7: XRD Pattern of Solution Treated Sample at 1020⁰C.

In addition, some secondary lamellar alpha phase and martensitic phase (α'') was precipitated in the β -matrix. X-Ray diffraction pattern analysis of the sample verified the microstructure evolution with large β peaks, where the volume fraction of β -phase was in the range of 79%, and low α_s peaks. Figure 7 shows the X-Ray diffraction pattern of the treated sample at 1020°C.

Mechanical Properties

Figure 8 shows hardness of as-received, solution treated below and above β -transus samples. The highest hardness of 492HV30 was reported for solution treated sample above β -transus due to precipitation of secondary lamellar alpha phase and small lathes of martensitic phase (α'') in β -matrix. The lowest hardness of 349HV30 was reported for the as-received sample due to presence of high amount of primary α -phase in the structure. Meanwhile, the sample treated at 920°C showed hardness value of 453HV30 due to its structure that contained α , β and α_s . It could be concluded that the precipitated phases (α_s & α'') at β -phase had a big role in increasing hardness of the studied TC21 titanium alloy.

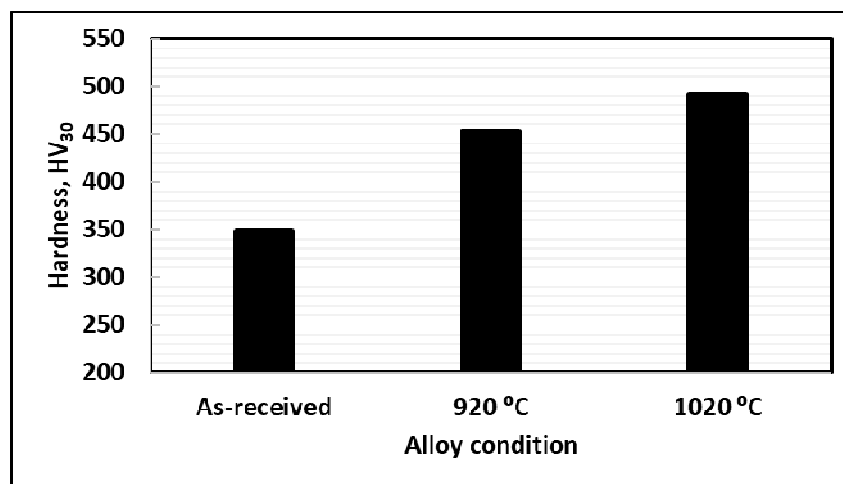


Figure 8: Hardness of the Investigated TC21 Titanium Alloy at Different Conditions.

Figure 9 shows tensile properties of as-received and solution treated samples at 920°C and 1020°C. The results showed that the highest tensile strength of 1447 MPa was recorded for the sample solution treated at 920°C due to strengthening the β -matrix with fine secondary lamellar α -platelets (α_s). However, the lowest strength of 1100 MPa was reported for the as-received samples because of its structure that consisted of equiaxed structure of $\alpha+\beta$. Mean while, the samples solution treated at 1020°C showed at ensile strength of 1391 MPa which is lower than the samples treated at 920°C because of forming fine martensitic structure (α'') in β -matrix. This fine (α'') caused embrittlement and sites for crack initiation during the tensile test, which in turn decreased the strength comparing to the samples treated at 920°C. The effect of microstructure on ductility of the studied TC21 titanium alloy under the three different conditions is shown in Fig.9 (b). The as-received and treated samples at 920°C showed relatively the same ductility of about 8%. This is because the as-received sample contained large amount of α -phase distributed homogenously in the structure. And the sample treated at 920°C have mostly β structure with some fine secondary lamellar α -plates (α_s) imbedded in the β -matrix. However, the sample treated at 1020°C showed the lowest ductility of 1.5% due to the large grains of β -structure and also existing of fine martensitic phase (α'') precipitated in β -matrix. This fine α'' causes embrittlement in the structure and hence decreased the ductility.

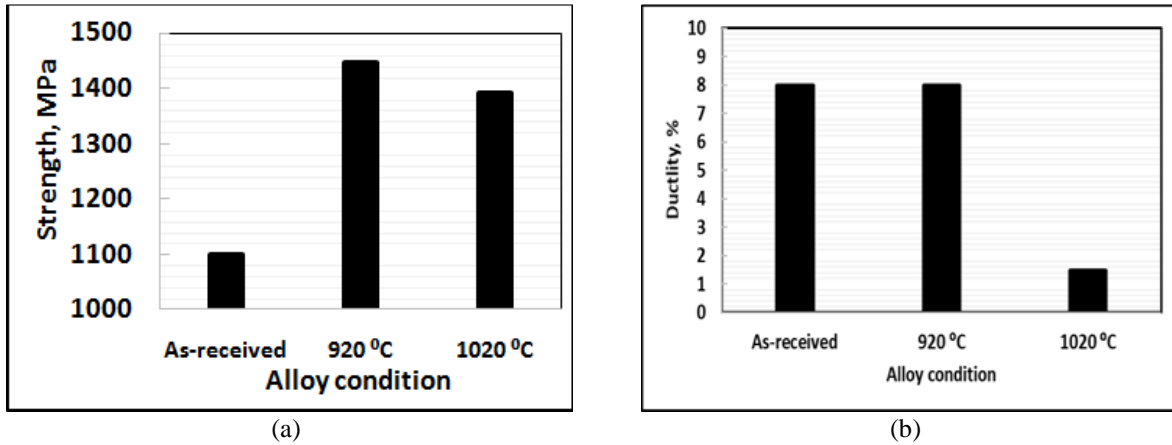


Figure 9: Tensile Properties of TC21 Titanium Alloy at Different Conditions; (a) Tensile Strength and (b) Ductility.

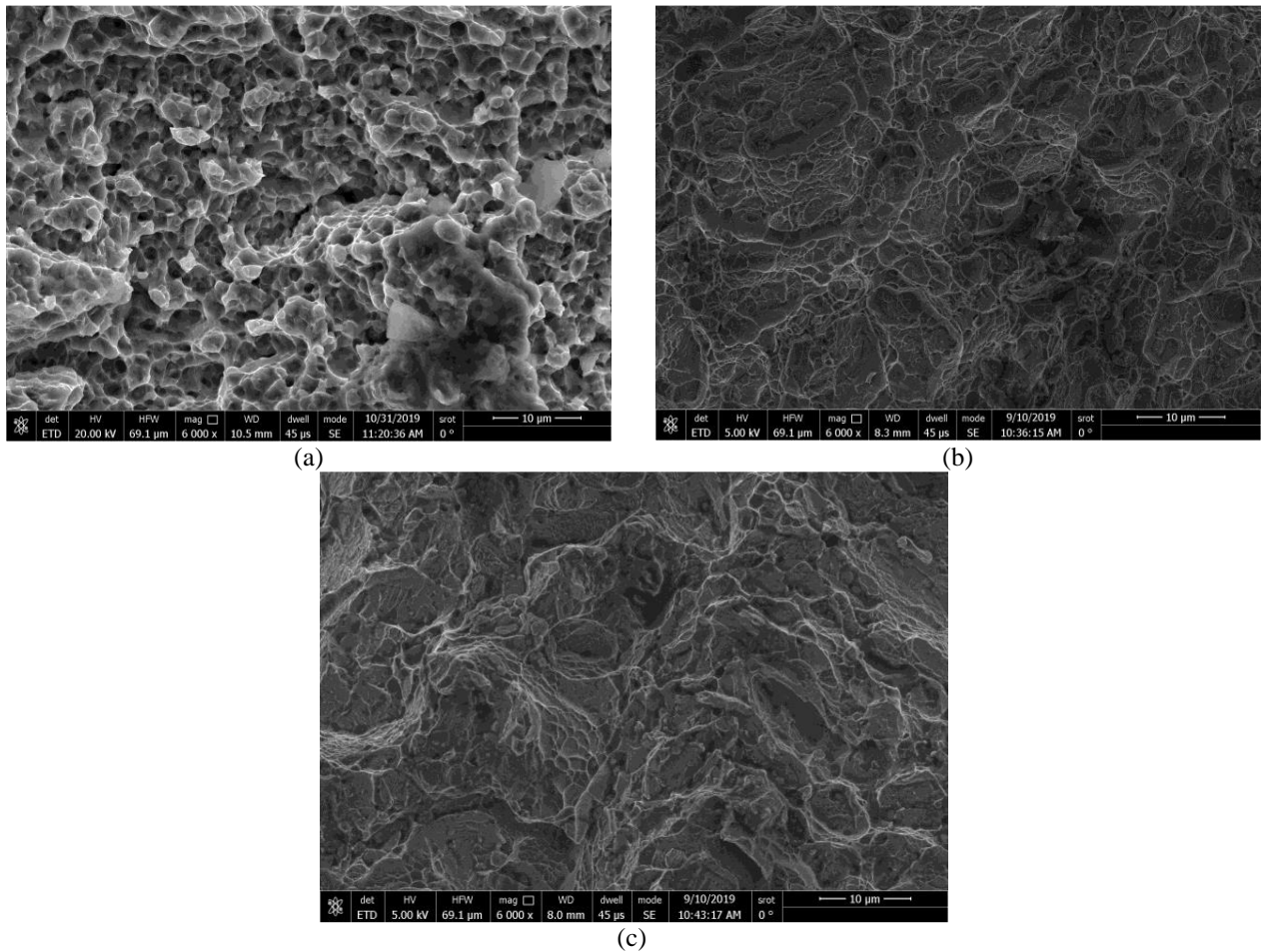


Figure 10: Fractography of Tensile Samples at Three Different Conditions; (a) As Received, (b) Treated 920 °C and (c) Treated at 1020 °C.

The fracture surfaces of the three studied TC21 samples are shown in Fig.10. The fracture surface of the as-received sample revealed large areas of dimples that indicated high ductility of the sample as shown in Fig.10 (a). The sample treated at 920 °C showed quasi-cleavage fracture surface with large amount of dimples that is referred to the α_p -phase existing in the structure; Fig.10 (b). However, the sample treated at 1020 °C illustrated a cleavage fracture with very low amount of ductile areas; Fig.10 (c), which confirms the obtained practical result of 1.5% ductility.

CONCLUSIONS

In this study, TC21 titanium alloy in annealed condition with an equiaxed $\alpha+\beta$ structure was solution treated at temperature below β -transus (920°C, 15 min) and temperature above β -transus (1020°C, 15 min, WQ). Aging was applied for both groups of samples (600°C, 4h, AC). The concluding remarks of this study can be summarized as follow:

- A structure consisted of α , β and α_s was obtained after solution treatment of TC21 titanium alloy at 920°C. While large β -grains imbedded in α_s and martensite α'' was obtained when samples treated at 1020°C.
- Maximum hardness of 492HV₃₀ was obtained for the samples treated at 1020°C due to existing of α_s and α'' in the structure and the minimum hardness of 349 HV₃₀ was reported for the as-received condition due to existing of a large amount of α_p -phase (65%) in the structure.
- Optimum tensile strength (1447MPa) and ductility (8%) was reported for the sample treated at 920°C as a result of existing fine grains of α , β and precipitated α_s in its structure.
- Fracture surfaces of as-received and treated sample at 920°C revealed high amount of dimples resulting from α -phase existing in the structure. However, the sample treated at 1020°C showed cleavage fracture due to existing of fine α'' in the structure.

REFERENCES

1. G. Lütjering, J. C. Williams, "Titanium", second edition, Springer, Berlin Heidelberg, New York, (2007).
2. K. M. Ibrahim, A. M. EL-Hakeem, R. N. Elshaer, "Microstructure and mechanical properties of cast and heat treated Ti-6.55 Al-3.41 Mo-1.77 Zr alloy", *Transactions of Non ferrous Metals Society of China*, vol. 23, (2013), pp.3517-3524.
3. LIU Hui-jie, FENG Xiu-li. *Microstructures and interfacial quality of diffusion bonded TC21 titanium alloy joints [J]. Transactions of Nonferrous Metals Society of China*, 2011, 21: 58-64.
4. ZHU Zhi-shou, WANG Xin-nan, GU Wei, CHEN Ming-he. *Study on high temperature deformation behaviors of new type TC21 titanium alloy [J]. Materials China*, 2009, 28: 51-55.
5. H. Shao, Y. Zhao, P. Ge, W. Zeng, "Crack initiation and mechanical properties of TC21 titanium alloy with equiaxed microstructure", *Material science & engineering A*, vol. 586, (2013), pp.215-222.4.
6. C. Tan, Q. Sun, L. Xiao, Y. Zhao, J. Sun "Cyclic deformation and microcrack initiation during stress controlled high cycle fatigue of a titanium alloy", *Materials Science & Engineering A*, vol.711 (2019), pp. 212-222.
7. G. Li, S. Qu, S. Guan, F. Wang, "Study on the tensile and fatigue properties of the heat- treated HIP Ti-6Al-4V alloy after ultrasonic surface rolling treatment", *Surface & coating technology*, vol. 379, (2019), pp. 124971.
8. T. Kakiuchi, R. Kawaguchi, M. Nakajima, M. Hojo, K. Fujimoto, Y. Uematsu, "Prediction of fatigue limit in additively manufactured Ti-6Al-4V alloy at elevated temperature", *International journal of fatigue*, vol. 126, (2019), pp. 55-61.
9. Z. Shi, H. Guo, R. Liu, X. Wang, Z. Yao, "Microstructure and mechanical properties of TC21 titanium alloy by near-isothermal forging", *Transactions of nonferrous metals society of china*, vol. 25, (2015), pp. 72-79.

10. C. Tan, X. Li, Q. Sun, L. Xiao, Y. Zaho, J. Sun, "Effect of α -phase morphology on low cycle fatigue behavior of TC21 alloy", *International journal of fatigue*, vol. 75, (2015), pp. 1-9.
11. N. Baohua, Z. Zihua, O. Yongzhong, C. Dongchu, C. Hong, S. Haibo, L. Shu, "Effect of LCF pre-damage on very high cycle fatigue behavior of TC21 titanium alloy", *International journal of fatigue*, vol. 1, (2017), pp. 10-182.
12. B. Nie, D. Chen, Z. Zhao, J. Zhang, Y. Meng, G. Gao, "Notch effect on the fatigue behavior of a TC21 titanium alloy in very high cycle regime", *Applied sciences*, vol. 8, (2018), 1614
13. R. N. Elshaer, K.M. Ibrahim, A.F. Barakat, R.R. Abbas, Determination of phase transformation for TC21 Ti-alloy by dilatometry method, *Open Journal of Metal*, vol. 9, (2019), pp. 1-10.
14. X. Peng, H. Guo, Z. Shi, C. Qjn, Z. Zhao, "Microstructure characterization and mechanical properties of TC4-DT titanium alloy after thermomechanical treatment", *Transactions of nonferrous metals society of china*, vol. 24, (2014), pp. 682-689.
15. S. Zhang, Y. Liang, Q. Xia, M. Ouzhao, "Study on Tensile Deformation Behavior of TC21 Titanium Alloy", *JMEPEG*, vol. 28, (2019), pp. 1581–1590.